Available online at www.sciencedirect.com
ScienceDirect
Journal of Photochemistry and Photobiology A: Chemistry 197 (2008) 115–123
Journal of Photochemistry and Photobiology A:Chemistry
www.elsevier.com/locate/jphotochem

Photoassisted dehalogenation and mineralization of chloro/fluoro-benzoic acid derivatives in aqueous media

Hisao Hidaka [a,**], Haruo Honjou [a], Takayoshi Koike [a], Yoshihiro Mitsutsuka [a], Toshiyuki Oyama [a], Nick Serpone [b,*]

[a] *Frontier Research Center for the Global Environment Science, Meisei University, 2-1-1, Hodokubo, Hino, Tokyo 191-8506, Japan*
[b] *Departimento di Chimica Organica, Università di Pavia, Via Taramelli 10, Pavia 27100, Italy*

Received 7 November 2007; received in revised form 11 December 2007; accepted 13 December 2007
Available online 23 December 2007

Abstract

The photoassisted dehalogenation and mineralization of chloro/fluoro-benzoic acid derivatives occurring at the TiO_2/H_2O interface under oxygen-saturated and UV-light exposure were examined by UV absorption spectroscopy, ion chromatography and time-of-flight (TOF) mass spectrometry to identify intermediate products. Contrary to defluorination, dechlorination occurred readily, presumably because of the weaker C–Cl bond relative to the C–F bond. Photodegradation through aromatic ring cleavage also occurred fairly rapidly followed by the ultimate evolution of CO_2 gas through prior formation of formate and bicarbonate species. When negative inductive effect groups, such as the chloro and fluoro groups, are positioned *ortho* and *para* to the carboxylic acid group, as in the 2Cl–4F–BA, 2Cl–6F–BA, and 4Cl–2F–BA derivatives, dechlorination was faster than when the chloro group was *meta* to the carboxylic acid group. Theoretically calculated frontier election densities and point charges of all the atoms in the Cl/F–BA derivatives are given. Plausible steps in the photo-degradation/-mineralization of these substrates are discussed.

Keywords: Chlorinated aromatics; Fluorinated aromatics; Chloro/fluoro-benzoic acids; TiO_2 photoassisted degradation and mineralization; Time-of-flight mass spectrometry

1. Introduction

The photoassisted degradation of various organic substances occurring through the mediation of TiO_2 (mostly anatase) from the standpoint of wastewater treatment has received considerable attention. Discharge of fluorinated organics into the natural environment either causes accumulation of such pollutants [1,2] and/or the possible condensation of such substrates in living bodies [3]. The problems of disposing of such hard-to-degrade substances, therefore, are significant for the protection and remediation of aquatic environments (e.g., lakes, rivers).

The first report on the photoassisted degradation of organic compounds by TiO_2 was the study by Kato and Mashio [4] in 1964. Only some decades later did studies on TiO_2-photoassisted degradations of, for example, chlorinated aromatics [5–12], chlorinated aliphatics [13–15] and fluorinated aliphatics [16–18] appear. Although relationships between chemical structures and degradation rates were investigated in such substrates, there nonetheless remain several unsolved problems of the degradation process. For instance, environmentally persistent compounds such as fluoride-bearing versus chloride-bearing aromatics (also cyanuric acid) present a formidable challenge in their disposal, even indirectly by the strongly oxidative $^{\bullet}OH$ radicals (or directly by the holes) photogenerated subsequent to irradiation of TiO_2 in aqueous media [19,20]. This probably arises because of differences in carbon–halogen bond dissociation energies (BDE). For instance, the BDE of C–F bonds (524 kJ/mol for aromatics and 472 kJ/mol for aliphatics) is significantly greater than the bond energy of C–Cl bonds (396 kJ/mol for aromatics and 342 kJ/mol for aliphatics).

The adsorption behavior of substances on TiO_2 surfaces (powders or thin films) and the position(s) of attack of such substances by $^{\bullet}OH$ radicals are important factors that affect the dynamics and the nature of intermediates produced toward the final products (typically CO_2, H_2O and innocuous anions) [21].

* Corresponding author. Tel.: +39 0382 98 73 16; fax: +39 0382 98 73 23.
** Co-corresponding author.
E-mail addresses: hidaka@epfc.meisei-u.ac.jp (H. Hidaka), nick.serpone@unipv.it (N. Serpone).

1010-6030/$ – see front matter © 2007 Elsevier B.V. All rights reserved.
doi:10.1016/j.jphotochem.2007.12.013

Primary events in the initial stages of decomposition can generally be inferred through MOPAC calculations of point charges and frontier electron densities prior to an examination of the experimental photodegradation process [22,23].

This article reports on the photoassisted degradation of four chloro/fluoro-benzoic acids in aqueous TiO_2 dispersions. In particular, we examine in some detail the dependence of the substituent positions of the chloro and fluoro groups in the benzoic acid structure on the degradation dynamics. Chloro and fluoro groups on organic molecules can be converted into chloride ions and fluoride ions as final mineralized products, respectively, along with carbon dioxide and water for the carbonaceous residue. Results indicate that although dechlorination was easily achieved, defluorination proved more difficult. Identification of intermediate species during the photoassisted degradative process of chloro/fluoro-bearing aromatic substrates was carried out using both LC–MS and TOF-MS mass spectral techniques. In addition, the extent of adsorption of the substrates on the TiO_2 surface, aromatic ring cleavage, quantity of CO_2 evolved, and the extent of dechlorination are reported against illumination time. Results are compared for the different halogenated derivatives of benzoic acid. A plausible mechanism of the degradation is also proposed.

2. Experimental

2.1. Chemicals and reagents

The structures of the aromatic substrates examined herein and subjected to photodegradation are shown in the structures below. Also shown are the pK_as of the benzoic acid derivatives that were estimated using Hammett's rule at 25 °C [24,25]. The pK_a of the parent benzoic acid (BA) is 4.19, whereas the pK_a of the chlorinated benzoic acid, 2Cl–BA, is 2.92. All the chloro/fluoro-benzoic acid derivatives were supplied by Tokyo Kasei Co. and were used as received. Benzoic acid (BA) and 2-chlorobenzoic acid (2Cl–BA) were supplied by Wako Pure Chem. Ind.; they were employed as standard samples. The photomediator was TiO_2 Degussa P-25 (particle size 20–30 nm by microscopic methods; specific surface area, ca. 53 $m^2\,g^{-1}$ by BET techniques; 83% anatase and 17% rutile by XRD).

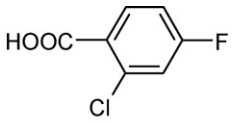

2-chloro-4-fluorobenzoic acid (2Cl-4F-BA) ; pKa = 2.86

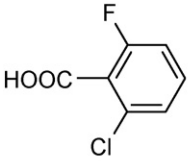

2-chloro-6-fluorobenzoic acid (2Cl-6F-BA) ; pKa = 1.99

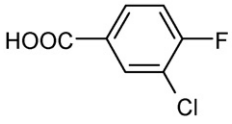

3-chloro-4-fluorobenzoic acid (3Cl-4F-BA) ; pKa = 3.76

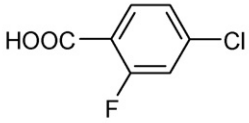

4-chloro-2-fluorobenzoic acid (4Cl-2F-BA) ; pKa = 3.04

2.2. Photoassisted degradation and analytical procedures

Fifty milliliters of the aqueous dispersion was contained in a tightly closed 127-mL Pyrex cylindrical batch photoreactor irradiated externally with a 75-W high-pressure Hg lamp (Toshiba SHL-100UVQ2). A magnetic stirrer guaranteed a satisfactory suspension uniformity of the reacting mixture that had been pre-saturated with O_2 gas by purging with pure oxygen at atmospheric pressure for ca. 0.5 h prior to irradiation. During the course of the photodegradation, the photoreactor was air-cooled with a fan; the suspension temperature was ca. 313 K (~40 °C). The TiO_2 loading was 2.0 $g\,L^{-1}$. Unless noted otherwise, the initial concentrations of the chlorinated/fluorinated benzoic acid derivatives were 0.10 mM, and the initial pH of the aqueous TiO_2 dispersion was 3.9 ± 0.1. The light irradiance impinging on the suspension was ca. 2 mW cm^{-2} in the wavelength range 310–400 nm (maximal lamp emission, 360 nm; Topcon UVR-2 radiometer).

The temporal evolution of CO_2 was assayed during the photoreaction by means of a Shimadzu GC-8AIT Gas Chromatograph equipped with a packed Shimadzu Porapack Q 80–100 column (for CO_2 evolution) linked to a TCD detector; helium was the carrier gas. Formation of chloride and fluoride ions was assayed by a high performance liquid chromatographic system (HPLC; Jasco) equipped with a CD-5 conductivity detector and a Shodex anionic (I-524) column. The eluent was a solution of phthalic acid (2.5 mM) and tris(hydroxylmethyl)-aminomethane (2.3 mM). Analyses were performed after removal of TiO_2 particles by centrifugation and eventual filtration with an Advantec 0.2 μm PTFE filter.

Intermediate products from the photodegradation process were analyzed by time-of-flight mass spectral techniques (TOF-MS) with a JEOL TOF CS JMS-T100CS mass spectrometer (applied voltage for electron spray ionization ESI was −2000 V; detection voltage was 2600 V; temperature of vaporization of the degraded sample in the methanolic aqueous medium was 100 °C; ring lens voltage was −15 V, while that of orifice 1 was −15 V and that of orifice 2 was −7 V); subsequent to a tenfold dilution of the degraded solution with methanol, the sample was injected into the probe at 10 μL min^{-1}. Note that LC–MS techniques (Agilent HP 1100 mass spectrometer, using the combined atmospheric pressure chemical ionization–electron spray ionization

(APCI-ESI)) were also utilized to examine the nature of the intermediates that led to the identification of *p*-fluorobenzoic acid, not otherwise observed by the TOF-MS methods (for details of procedures used in the LC–MS technique see ref. [26]). In all cases, the data were recorded in the negative-ion mode.

2.3. Point charge and electron density calculations

Molecular orbital calculations were performed by the parametric method 3 (PM3) with application of the Window-based MOPAC program. All geometrical parameters of the four halogenated benzoic acid derivatives were calculated using the Broyden–Fletcher–Goldfarb–Shannon algorithm incorporated in the program for optimization, with the minimum energy obtained at the AM1 level. Geometries of the substrates examined in aqueous solution were compared to those obtained in the gas phase by conductor-like screening model orbital (COSMO) and electrostatic potential (point charge) calculations. The COSMO procedure generated a conducting polygonal surface around the system at van der Waal's distances. Standard values used herein were the number of geometrical segments per atom (NSPA = 60); the dielectric constant was taken as 78.4 at 25 °C (in water). Initial positions of the •OH radical attack are described in terms of frontier electron densities of the substituent groups and the phenyl carbons, whereas the possible modes of closest approach of the benzoic acid molecules to the TiO_2 particle surface are inferred from the calculated point charges.

3. Results and discussion

3.1. Photoassisted oxidative degradation

A multiply substituted benzene structure brings about aromatic $\pi \rightarrow \pi^*$ transitions of the broad E-band (195 nm) from the ethylenic moieties that display the highest molar extinction coefficient, and a B-band (230 nm) from the benzoic acid function that displays a relatively smaller coefficient [27].

The experimental absorption spectrum of the parent substrate benzoic acid (BA) exhibited bands at 196 nm ($\varepsilon = 18{,}200\ M^{-1}\ cm^{-1}$) and at 230 nm ($\varepsilon = 6500\ M^{-1}\ cm^{-1}$). After 15 min of irradiation, the intensity of the 196-nm band decreased, whereas the 230-nm band disappeared entirely within 2 h of illumination. The other parent substrate 2-chlorobenzoic acid (2Cl–BA) displayed a band at 198 nm ($\varepsilon = 2000\ M^{-1}\ cm^{-1}$) and an unresolved band around 220–230 nm; the latter also disappeared completely with time. The time-evolving UV-

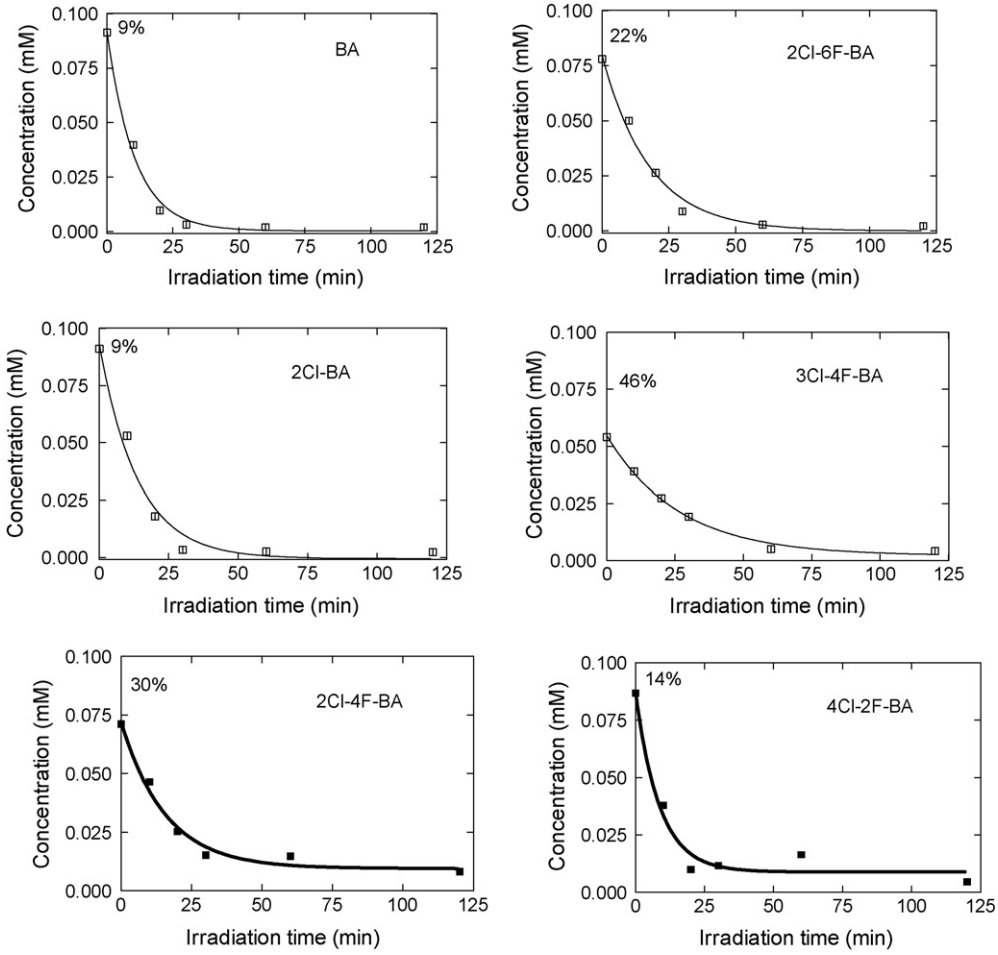

Fig. 1. First-order temporal concentration decrease for the benzoic acid derivatives (0.1 mM; 50 mL) in the presence of TiO_2 particles (100 mg) under UV light irradiation (values in percent indicate extent of adsorption in the dark).

Table 1
Rate constants of aromatic cleavage, CO_2 evolution and chloride ion formation; normalized constants relative to the degradation of 2-chlorobenzoic acid (2Cl–BA) are also shown.

	Ring opening k_{ring} (10^{-2} min^{-1})	$\frac{k}{k_{2Cl-BA}}$	CO_2 evolution k_{CO_2} (10^{-2} min^{-1})	$\frac{k}{k_{2Cl-BA}}$	Dechlorination k_{Cl^-} (10^{-2} min^{-1})	$\frac{k}{k_{2Cl-BA}}$
2Cl–4F–BA	6.37	0.88	6.37	1.32	8.44	0.84
2Cl–6F–BA	5.66	0.78	6.24	1.29	8.09	0.81
3Cl–4F–BA	3.78	0.52	5.27	1.09	6.24	0.62
4Cl–2F–BA	11.5	1.59	7.17	1.48	7.79	0.78
2Cl–BA	7.23	1.00	4.83	1.00	10.0	1.00
BA	9.56	1.32	3.20	0.66	–	–

absorption features of 2Cl–4F–BA were strikingly similar to the features exhibited by the 2Cl–BA sample.

The initial absorption spectrum of the 2Cl–6F–BA derivative exhibited a band maximum at 200 nm and a shoulder around 220–230 nm. The intensity of these two features decreased with increasing irradiation time. A similar tendency was observed during the photodegradation of the 3Cl–4F–BA derivative. Similarly, the absorption spectrum of the 4Cl–2F–BA substrate showed bands at 195 nm ($\varepsilon = 19{,}000\ M^{-1}\ cm^{-1}$), 230 nm ($\varepsilon = 7500\ M^{-1}\ cm^{-1}$) and another around 275 nm ($\varepsilon \sim 2500\ M^{-1}\ cm^{-1}$). The short wavelength band decreased in intensity, whereas the 230-nm and the 275-nm bands were no longer perceptible after only 15 min of UV irradiation of the TiO_2 dispersion.

The time-dependent photoinduced transformations of the BA parent substrate and the five halogenated benzoic acid derivatives are illustrated in Fig. 1; the extent of adsorption of the substrates on the TiO_2 surface prior to irradiation followed the trend: 3Cl–4F–BA (46%) > 2Cl–4F–BA (30%) > 2Cl–6F–BA (22%) > 4Cl–2F–BA (14%) > 2Cl–BA=BA (9%). The strong variations in the extent of adsorption of these substrates on the TiO_2 surface must be viewed in terms of competing effects between the point charges of the substituent groups along with the electronic and steric factors. The decrease of the short wavelength spectral band intensities that we attribute to a ring-opening process followed first-order kinetics with the rates reported in Table 1. Also given are the relative rates with respect to the standard 2Cl–BA substrate. Photodegradation was incomplete for the 2Cl–4F–BA and 4Cl–2F–BA substrates. Kinetics of ring-opening of the halogenated benzoic acid derivatives (and BA) followed the order: 4Cl–2F–BA > BA > 2Cl–BA > 2Cl–4F–BA > 2Cl–6F–BA > 3Cl–4F–BA.

The mineralization yields, expressed as % CO_2, after 2 h of UV irradiation are displayed in Fig. 2. The quantity of CO_2 evolved after this period followed the order 2Cl–BA (75%) > BA (70%) > 3Cl–4F–BA (61%) ~ 2Cl–4F–BA (59%) > 2Cl–6F–BA (54%) ~ 4Cl–2F–BA (52%), whereas the dynamics of CO_2 evolution in the photodecomposition of the chloro/fluoro-benzoic acids tended to follow the trend 4Cl–2F–BA > 2Cl–4F–BA = 2Cl–6F–BA > 3Cl–4F–BA. The rate of CO_2 evolution for the F-free benzoic acid (2Cl–BA) and the halogen-free benzoic acid (BA) substrates were about 1.5–2-fold slower (Table 1). Evidently, the F-bearing benzoic acids can be mineralized more easily than the F-free benzoic acids.

The temporal course of the photoinduced dechlorination during the photodegradation of halogenated benzoic acid derivatives with UV irradiation time is illustrated in Fig. 3. The retention time of the HPLC signal for the chloride ion was 4.01 min; that of the fluoride ion was 2.67 min. Defluorination was inconsequential during the same time period as dechlorination. Even after 72 h of irradiation the quantity of fluoride was negligible. Note that fluoride ions tend to adsorb strongly on the TiO_2 surface [28] so that a small quantity of F^- ions produced would not have been observed experimentally. Nonetheless, no defluorinated benzoic acid intermediates were observed by the mass spectral techniques (see below). Dechlorination of the 2Cl–BA substrate was nearly quantitative reaching about 98% within ca. 30 min of irradiation, whereas dechlorination of the

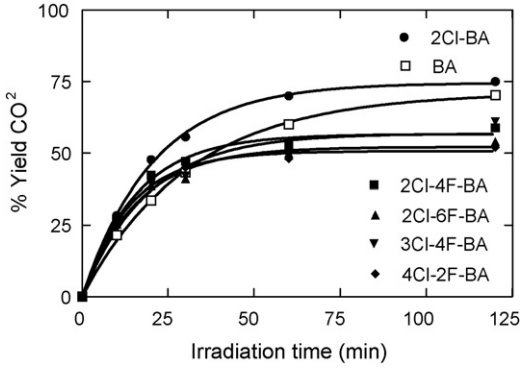

Fig. 2. Temporal CO_2 evolution in the photodegradation of benzoic acid derivatives. Experimental conditions same as those described in Fig. 1.

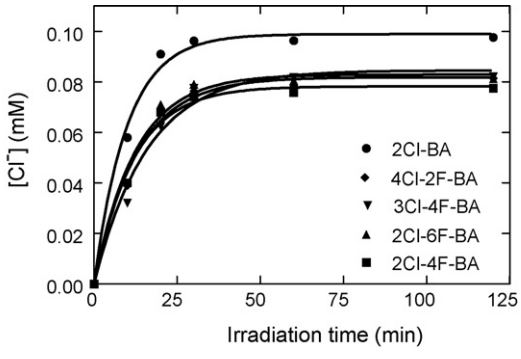

Fig. 3. Temporal formation of chloride ions in the photodegradation of the benzoic acid derivatives; experimental conditions same as those described in Fig. 1.

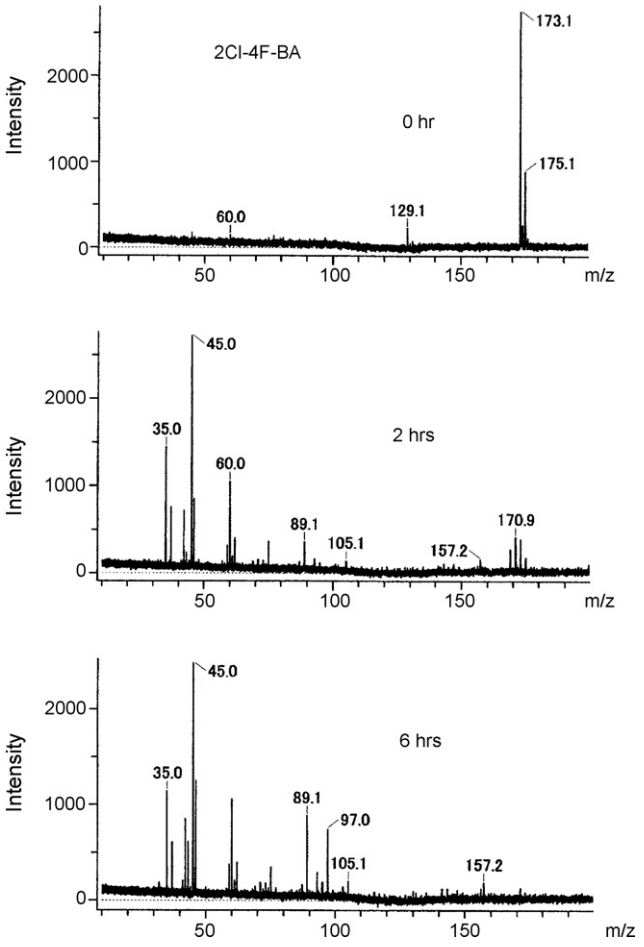

Fig. 4. Time-of-flight mass spectral fragmentation patterns for the 2Cl–4F–BA derivative recorded at time 0, 2 and 6 h of UV irradiation of the dispersion.

2Cl–4F–BA, 2Cl–6F–BA, 3Cl–4F–BA and 4Cl–2F–BA systems attained ca. 80%, regardless of the positions of the chloro and fluoro groups. First-order rates of formation of chloride ions for all the chlorinated substrates are also reported in Table 1; formation kinetics of chloride ions varied as 2Cl–BA > 2Cl–4F–BA > 2Cl–6F–BA > 4Cl–2F–BA > 3Cl–4F–BA.

Comparison of the dynamics of dechlorination and aromatic ring cleavage of Table 1 shows that dechlorination was somewhat faster than ring opening, except for the 4Cl–2F–BA derivative for which dechlorination ($k = 7.79 \times 10^{-2}$ min^{-1}) was slower than ring opening ($k = 11.5 \times 10^{-2}$ min^{-1}). Moreover, evolution of CO_2 in the photomineralization of all chlorinated benzoic acid substrates was slower than dechlorination and in some cases (4Cl–2F–BA, 2Cl–BA and BA) slower than aromatic ring opening.

3.2. Identification of intermediates

Intermediates formed during the photodegradation of the benzoic acid substrates to aid in inferring a plausible mechanism were identified from their TOF-MS mass spectral patterns illustrated in Fig. 4 for the 2Cl–4F–BA case. Soft ionization used to measure the exact mass numbers of intermediate species to distinguish temporally between a photooxidative process and an ionization process was also carried out by TOF-MS techniques. Since rapid vaporization is done by the electron spray ionization (ESI) procedure, the accuracy of the mass numbers of the photodegradative products is remarkably high.

Prior to illumination ($t = 0$) the mass spectral fragmentation pattern of the parent carboxylate form of 2Cl–4F–BA was observed at $m/z = 173.1$ in the negative-ion mode (the peak at 175.1 is consistent with the presence of Cl with its two isotopes). The relatively weak signal of 1-chloro-3-fluorobenzene formed from the decarboxylated parent substrate by electron-spray ionization was observed at $m/z = 129.1$ along with a mass spectral peak at $m/z = 60.0$ that we attribute to the presence of the HCO_3^- anion.

After 2 h of UV illumination, the mass spectral fragmentation pattern revealed a weak signal of 2Cl–4F–BA at $m/z = 173.1$ and a new peak of a deprotonated carboxylate form of 2Cl–4F–BA observed at ca. $m/z = 170.9$. New mass peaks belonging to 2-chloro-4-fluorobenzaldehyde ($m/z = 157.2$), 4-fluorobutanoic acid ($m/z = 105.1$), 3-fluoroacrylic acid ($m/z = 89.1$), 3-fluoropropanal ($m/z = 75.1$), bicarbonate ($m/z = 60.0$) and formate ($m/z = 45.0$) were also observed. Formation of Cl^- ions was seen at $m/z = 35.0$ and 37.0 in the appropriate ratio of the chlorine isotopes. The fragmentation pattern after 6 h of UV irradiation of the aqueous TiO_2 dispersion was similar to that after the 2-h irradiation period, except for the occurrence of the additional intermediate 1-fluoro-1,3-pentadiene at $m/z = 97.0$. No mass spectral peak of the original 2Cl–4F–BA substrate was seen after the 6-h period, indicating total degradation had occurred by this time and confirming the results of Fig. 1.

3.3. MOPAC calculated point charges and electron densities and plausible photodegradation steps of the Cl/F–BA derivatives

Point charges and frontier electron densities in the gas phase and in the aqueous phase for the four halogenated benzoic acids calculated by the MOPAC methodology are listed in Table 2. The O_8 and O_9 atoms possess the largest negative point charges in both gas and aqueous phases. Accordingly, adsorption of all the benzoic acid homologs on the TiO_2 surface should occur preferentially through the carboxylate groups. A plausible, albeit partial oxidation mechanism for the degradation of 2Cl–4F–BA can be proposed (Scheme 1) on the basis of the mass spectral patterns in Fig. 4. We need not emphasize that $^{\bullet}OH$ radicals are the primary oxidizing agents in photodegradations of organics as already reported extensively in the literature when TiO_2 is activated by UV irradiation [19,21,29].

Comparison of MOPAC calculations done for the gas phase with those estimated in the water phase also showed (but not reported) that chemical bonds between aromatic carbons and ring substituents of a substrate are lengthened, since the substrate lies in the bulk space surrounded by water molecules. Accordingly, differences between values of point charges and electron densities can become significant. In other words, positive values become more positive, whereas negative values become more negative in the aqueous phase as confirmed by the data of Table 2.

Table 2
Point charges and frontier electron densities of each benzoic acid substrate in the gas phase and in the presence of a water phase (significant values are illustrated in italic boldface)

2Cl–4F–BA

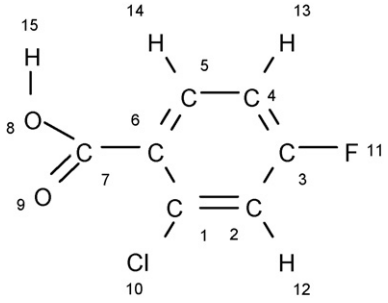

	Point charge		Electron density	
Atom	Gas	Water	Gas	Water
C1	−0.056	−0.050	4.056	4.050
C2	−0.157	−0.172	4.157	4.172
C3	0.113	0.125	3.887	3.875
C4	−0.143	−0.152	4.143	4.152
C5	−0.040	−0.001	4.040	4.000
C6	−0.171	−0.172	4.171	4.172
C7	0.407	0.568	3.593	3.431
O8	***−0.267***	***−0.325***	***6.267***	***6.325***
O9	***−0.326***	***−0.577***	***6.326***	***6.577***
Cl10	0.147	0.106	***6.853***	***6.894***
F11	−0.082	−0.109	***7.082***	***7.109***
H12	0.141	0.165	0.859	0.835
H13	0.131	0.156	0.869	0.845
H14	0.105	0.149	0.895	0.851
H15	0.197	0.288	0.803	0.712

2Cl–6F–BA

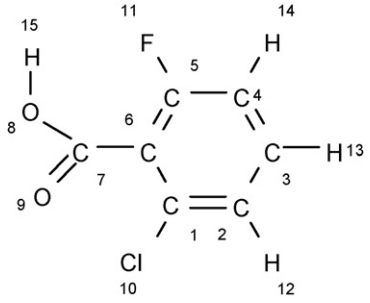

	Point charge		Electron density	
Atom	Gas	Water	Gas	Water
C1	−0.063	−0.055	4.063	4.055
C2	−0.134	−0.154	4.134	4.154
C3	−0.032	−0.015	4.032	4.015
C4	−0.142	−0.153	4.142	4.153
C5	0.097	0.147	3.903	3.853
C6	−0.180	−0.183	4.180	4.183
C7	0.414	0.574	3.586	3.426
O8	***−0.279***	***−0.336***	***6.280***	***6.336***
O9	***−0.333***	***−0.571***	***6.333***	***6.571***
Cl10	0.152	0.106	***6.848***	***6.894***
F11	−0.084	−0.086	***7.084***	***7.086***
H12	0.126	0.150	0.874	0.850
H13	0.113	0.138	0.887	0.862
H14	0.131	0.156	0.869	0.844
H15	0.214	0.283	0.786	0.717

3Cl-4F-BA

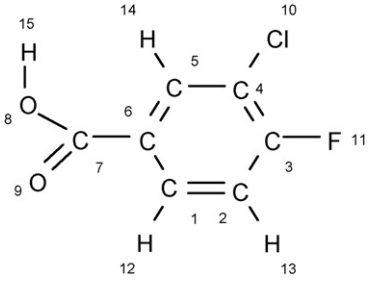

	Point charge		Electron density	
Atom	Gas	Water	Gas	Water
C1	−0.011	0.001	4.011	4.000
C2	−0.129	−0.141	4.130	4.141
C3	0.100	0.112	3.900	3.888
C4	−0.180	−0.203	4.180	4.203
C5	−0.055	−0.011	4.055	4.011
C6	−0.157	−0.163	4.157	4.163
C7	0.406	0.570	3.593	3.430
O8	***−0.265***	***−0.324***	***6.265***	***6.325***
O9	***−0.333***	***−0.582***	***6.333***	***6.582***
Cl10	0.123	0.103	***6.877***	***6.897***
F11	−0.076	−0.104	***7.076***	***7.104***
H12	0.133	0.141	0.867	0.859
H13	0.132	0.156	0.868	0.844
H14	0.115	0.158	0.885	0.842
H15	0.198	0.288	0.802	0.712

4Cl-2F-BA

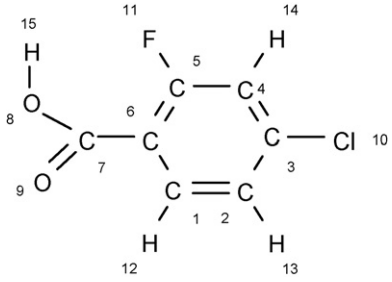

	Point charge		Electron density	
Atom	Gas	Water	Gas	Water
C1	0.001	0.010	3.999	3.990
C2	−0.125	−0.147	4.125	4.147
C3	−0.085	−0.076	4.085	4.076
C4	−0.142	−0.159	4.141	4.159
C5	0.101	0.154	3.899	3.846
C6	−0.187	−0.188	4.187	4.188
C7	0.415	0.575	3.585	3.425
O8	***−0.278***	***−0.336***	***6.278***	***6.336***
O9	***−0.339***	***−0.577***	***6.339***	***6.577***
Cl10	0.101	0.086	***6.899***	***6.914***
F11	−0.082	−0.085	***7.082***	***7.085***
H12	0.134	0.142	0.866	0.858
H13	0.128	0.151	0.871	0.849
H14	0.141	0.167	0.859	0.834
H15	0.215	0.283	0.785	0.717

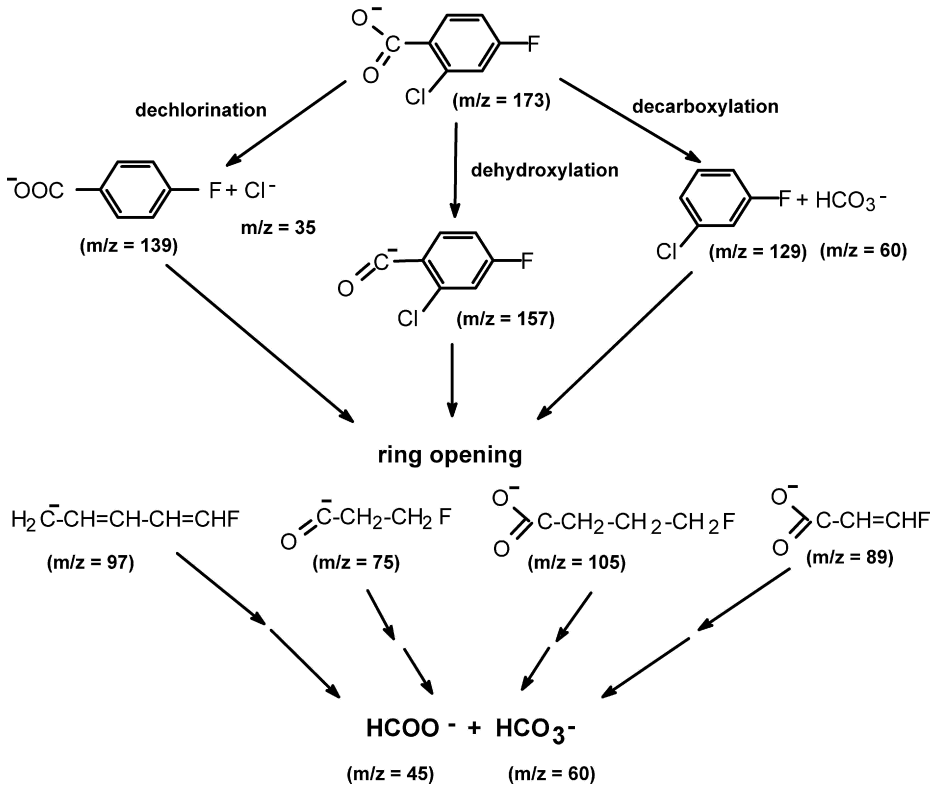

Scheme 1. Proposed oxidation pathway for the 2Cl–4F–BA benzoic acid derivative (*m/z* values obtain by TOF-MS in the negative ion mode). The presence of the 4-fluorobenzoate anion (*m/z* = 139) was detected by LC–MS mass spectrometry.

The •OH radical species generally attack substrates at positions of highest electron densities. It is noteworthy that these electron densities are greater in the aqueous phase than they are in the gas phase, no doubt the result of the polarizing effect of the polar water molecules. Thus, in principle, positions of •OH-radical attack should occur in both phases at the F_{11} and Cl_{10} positions in all the benzoic acid derivatives that exhibited the highest electron density, closely followed by the O_8 and O_9 atoms. However, it is also well known that •OH-radical addition to an aromatic ring occurs fairly rapidly [30], consistent with the notion that the total sum of electron densities of all the phenyl C_1 to C_6 carbons far outweigh the electron densities of the individual substituent atoms or groups. We do not preclude the possibility that the •OH radical positions itself at a phenyl ring carbon bonded to a substituent atom or group where the electron density was greatest. To the extent that the bond energy of the C–F bond is much greater than the C–Cl bond, it seems natural to expect the defluorination process to be impeded significantly. Accordingly, abstraction of Cl should be facilitated by addition of •OH radicals to the phenyl ring of the Cl/F–BA derivatives ultimately generating chloride ions (via displacement of Cl by OH and electron pickup by the former) in competition with decarboxylation and phenyl ring cleavage, and ultimately mineralization of the chloro/fluoro-benzoic acids.

Photoinduced dechlorination, degradation and mineralization can also occur by attachment of photogenerated conduction band electrons [31] to the phenyl rings on UV irradiation of TiO_2. Electrons so attached may then be localized at atoms with positive point charges of which the Cl substituent (see Table 2) is the more likely site for electron localization with subsequent release of chloride ions. Unfortunately, our available data cannot delineate between initial primary photooxidative (•OH radical addition) and photoreductive (electron attachment) steps. Accordingly, we speculate no further on the mechanistic details, except to indicate the intermediates identified that are reported in Scheme 1.

No cleavage of the aromatic C–F bond occurred under our conditions and within certain constraints on the basis of our experimental HPLC-ion chromatographic data and mass spectral results for the case of the 2Cl–4F–BA substrate illustrated in Fig. 4.

Dechlorination of 2Cl–4F–BA led to formation of the 4-fluorobenzoic acid intermediate (*m/z* = 139), identified by LC–MS techniques, whereas decarboxylation produced the 1-chloro-3-fluoro-benzene (*m/z* = 129) and bicarbonate (*m/z* = 60) intermediates. With a minor exception, dechlorination appears to be somewhat faster than photodegradation through ring cleavage and evolution of carbon dioxide (photomineralization). A curious finding involves the dehydroxylation of this Cl/F–BA derivative to yield the 2-chloro-4-fluorobenzaldehyde species at *m/z* = 157. Subsequent dechlorination and ring opening of these intermediates yield several chloride-free but fluoride-bearing aliphatic intermediates identified from their mass numbers: 4-fluorobutanoic acid (*m/z* = 105), 1-fluoro-1,3-pentadiene (*m/z* = 97), 3-fluoro-2-propenoic acid (i.e., 3-fluoroacrylic acid; *m/z* = 89), and 3-fluoro-propanal (*m/z* = 75). Further oxidation of

the latter fluorinated species yields ultimately formate species ($HCOO^-$; $m/z = 45$) on the way to carbon dioxide seen as bicarbonate (HCO_3^-; $m/z = 60$) under our mass spectral conditions.

4. Concluding remarks

The TiO_2-photoassisted dechlorination, decarboxylation and ultimate mineralization of chloro/fluoro-substituted benzoic acid derivatives (with Cl and F groups at various positions on the aromatic ring) to carbon dioxide have been examined by various chromatographic (HPLC-IC) and spectral methods (UV–vis, TOF-MS and LC–MS). Intermediates have been identified and have aided in inferring a reasonable, albeit incomplete mechanism. When negative inductive effect groups, such as the chloro and fluoro groups, are positioned *ortho* and *para* to the carboxylic acid group, as in the 2Cl–4F–BA, 2Cl–6F–BA, and 4Cl–2F–BA derivatives, dechlorination was faster than when the chloro group was positioned *meta* to the acid group. Degradation through ring opening followed by mineralization (i.e. evolution of CO_2) of these three substrates also appear to be faster than for the 3Cl–4F–BA system. Dechlorination tends to dominate initially. The relative positions of the halo groups on such halogenated aromatic pollutants bear on the kinetics. For instance, cleavage of the 4Cl–2F–BA phenyl ring is nearly twofold faster than the 2Cl–4F–BA analog, yet dechlorination is slightly slower for the former substrate no doubt due to the remote location of the chloro group from the TiO_2 surface where photoinduced processes are initiated.

Acknowledgments

Financial support from the Frontier Research Promotion Foundation and a Grant-in-Aid for Scientific Research (C) 17550145 by Japanese Ministry of Education, Culture, Sports, Science and Technology (to H.H.) for the works carried out in Japan. One of us (NS) thanks Prof. Albini and his group at the University of Pavia for their kind hospitality. The authors also thank Prof. T. Kurihara and Mr. T. Ohno for the MOPAC simulation studies, and Prof. T. Machinami and Dr. T. Fujimoto for the TOF-MS spectral measurements.

References

[1] C.M. Butt, S.A. Mabury, D.C.G. Muir, B.M. Braune, Prevalence of long-chained perfluorinated carboxylates in seabirds from the Canadian Arctic between 1975 and 2004, Environ. Sci. Technol. 41 (2007) 3521.
[2] N.L. Stock, V.I. Furdui, D.C.G. Muir, S.A. Mabury, Perfluoroalkyl contaminants in the Canadian Arctic: evidence of atmospheric transport and local contamination, Environ. Sci. Technol. 41 (2007) 3529.
[3] K.S. Kumar, Fluorinated organic chemicals: a review, Res. J. Chem. Environ. 9 (2005) 50.
[4] S. Kato, F. Mashio, TiO_2 photocatalyzed oxidation of tetraline in liquid phase, Kogyo Kagaku Zasshi (Jpn. Ind. Chem.) 67 (1964) 1136.
[5] J.H. Carey, J. Lawrence, H.M. Tosine, Photodechlorination of PCB's in the presence of titanium dioxide in aqueous suspensions, Bull. Environ. Contam. Toxicol. 16 (1976) 697.
[6] B.G. Oliver, E.G. Cosgrove, J.H. Carey, Effect of suspended sediments on the photolysis of organics in water, Environ. Sci. Technol. 13 (1979) 1075.
[7] M. Barbeni, E. Pramauro, E. Pelizzetti, E. Borgarello, M. Grätzel, N. Serpone, Photodegradation of 4-chlorophenol catalyzed by titanium dioxide particles, Nouv. J Chim. 8 (1984) 547.
[8] E. Pelizzetti, M. Barbeni, E. Pramauro, N. Serpone, E. Borgarello, M.A. Jamieson, H. Hidaka, Sunlight photodegradation of haloaromatic pollutants catalyzed by semiconductor particles materials, Chim. Ind. (Milan) 67 (1985) 623.
[9] R.W. Matthews, Photo-oxidation of organic material in aqueous suspensions of titanium dioxide, Water Res. 20 (1986) 569.
[10] R. Borello, C. Minero, E. Pramauro, E. Pelizzetti, N. Serpone, H. Hidaka, Photocatalytic degradation of DDT mediated in aqueous semiconductor slurries by AM1 simulated sunlight, Environ. Toxicol. Chem. 8 (1989) 997.
[11] J.-M. Herrmann, J. Motos, J. Disdier, C. Guillard, J. Laine, S. Malato, J. Blanco, Solar photocatalytic degradation of 4-chlorophenol using the synergistic effect between titania and activated carbon in aqueous suspension, Catal. Today 54 (1999) 255.
[12] J.P. Wilcoxon, Catalytic photooxidation of pentachlorophenol using semiconductor, J. Phys. Chem. B 104 (2000) 7334.
[13] A.L. Pruden, D.F. Ollis, Photoassisted heterogeneous catalysis: the degradation of trichloroethylene in water, J. Catal. 82 (1983) 404.
[14] H. Hidaka, K. Nohara, J. Zhao, N. Serpone, E. Pelizzetti, Photooxidative degradation of the pesticide permethrin catalyzed by irradiated TiO_2 semiconductor slurries in aqueous media, J. Photochem. Photobiol. A: Chem. 64 (1992) 247.
[15] H. Hidaka, H. Jou, K. Nohara, J. Zhao, Photocatalytic degradation of the hydrophobic pesticide permethrin in fluoro surfactant/TiO_2 aqueous dispersions, Chemosphere 25 (1992) 1589.
[16] R. Dillert, D. Bahnemann, H. Hidaka, Light-induced degradation of perfluorocarboxylic acid in the presence of titanium dioxide, Chemosphere 67 (2007) 785.
[17] H. Hori, Y. Takano, K. Koike, K. Takeuchi, H. Einaga, Decomposition of environmentally persistent trifluoroacetic acid to fluoride ions by a homogeneous photocatalyst in water, Environ. Sci. Technol. 37 (2003) 418.
[18] H. Hori, Y. Takano, K. Koike, S. Kutsuna, H. Einaga, T. Ibusuki, Photochemical decomposition of pentafluoropropionic acid to fluoride ions with a water-soluble heteropolyacid photocatalyst, Appl. Catal. B: Environ. 46 (2003) 333.
[19] G. Mills, M.R. Hoffmann, Photocatalytic degradation of pentachlorophenol on TiO_2 particles: identification of intermediates and mechanism of reaction, Environ. Sci. Technol. 27 (1993) 1681.
[20] J.-C. D'Oliveira, C. Guillard, C. Maillard, P. Pichat, Photocatalytic destruction of hazardous chlorine- or nitrogen-containing aromatics in water, J. Environ. Sci. Health A: Environ. Sci. Eng. 28 (1993) 941.
[21] M.A. Fox, M.T. Dulay, Heterogeneous photocatalysis, Chem. Rev. 93 (1993) 341.
[22] H. Hidaka, T. Koike, N. Serpone, Photocatalytic degradation of surfactants. XX. Photooxidation of sodium butylnaphthalenesulfonates, J. Oleo Sci. 52 (2003) 245.
[23] H. Hidaka, T. Koike, T. Kurihara, N. Serpone, Dynamics and mechanistic features in the photocatalyzed oxidation of disulfonated anionic surfactants on the surface of UV-irradiated titania nanoparticles, New J. Chem. 28 (2004) 1100.
[24] L.P. Hammett, The Effect of Structure upon the Reactions of Organic Compounds. Benzene Derivatives, J. Am. Chem. Soc. 59 (1937) 96.
[25] A. Streitwieser, C.H. Heathcock, E.M. Kosower, in: P.F. Corey (Ed.), Introduction to Organic Chemistry, fourth ed., Macmillan Publ. Co., New York, 1992.
[26] N. Watanabe, S. Horikoshi, K. Suzuki, H. Hidaka, N. Serpone, Mechanistic inferences of the photocatalyzed oxidation of chlorinated phenoxyacetic acids by electrospray mass spectral techniques and from calculated point charges and electron densities on all atoms, New J. Chem. 27 (2003) 836.
[27] E. Pretsch, P. Bühlmann, C. Affolter, Structure Determination of Organic Compounds, Table of Spectral Data, Springer, Germany, 2000, pp. 385.
[28] C. Minero, G. Mariella, V. Maurino, E. Pelizzetti, Photocatalytic transformation of organic compounds in the presence of inorganic anions. 1. Hydroxyl-mediated and direct electron-transfer reactions of phenol on a titanium dioxide-fluoride system, Langmuir 16 (2000) 2632.

[29] (a) N. Serpone, E. Pelizzetti (Eds.), Photocatalysis–Fundamentals and Applications, Wiley Interscience, New York, 1989;
(b) N. Serpone, E. Pelizzetti, H. Hidaka, Identifying primary events and the nature of intermediates formed during the photocatalyzed oxidation of organics mediated by irradiated semiconductors, in: D.F. Ollis, H. Al-Ekabi (Eds.), Photocatalytic Purification and Treatment of Water and Air, Elsevier, Amsterdam, The Netherlands, 1993, pp. 225–250.
[30] See for example the Notre Dame Radiation Laboratory Data Center's listings of $^{\bullet}$OH radical reactions with various aromatic substrates http://www.rcdc.nd.edu/compilations/Hydroxyl/oh.htm (accessed October (2007).
[31] (a) R. Terzian, N. Serpone, R.B. Draper, M.A. Fox, E. Pelizzetti, Pulse radiolysis of pentahalophenols: formation, kinetics, and properties of pentahalophenoxyl and dihydroxypentahalocyclohexadienyl radicals, Langmuir 7 (1991) 3081;
(b) N. Serpone, I. Texier, A.V. Emeline, P. Pichat, H. Hidaka, J. Zhao, Post-irradiation effect and reductive dechlorination of chlorophenols at oxygen-free TiO_2/water interfaces in the presence of prominent hole scavengers, J. Photochem. Photobiol. A: Chem. 136 (2000) 145.